BBA - Molecular Basis of Disease 1870 (2024) 167163

Contents lists available at ScienceDirect

BBA - Molecular Basis of Disease

journal homepage: www.elsevier.com/locate/bbadis

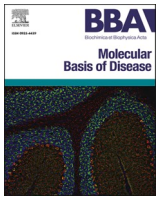

Transcriptomic analysis identifies dysregulated pathways and therapeutic targets in PMM2-CDG

Diana Gallego [a], Mercedes Serrano [b,c], Jose Cordoba-Caballero [d,e], Alejandra Gámez [a], Pedro Seoane [d,e], James R. Perkins [d,e,f,g], Juan A.G. Ranea [d,e,f,g,*], Belén Pérez [a,**]

[a] Centro de Diagnóstico de Enfermedades Moleculares, Centro de Biología Molecular-SO UAM-CSIC, Universidad Autónoma de Madrid, Campus de Cantoblanco, U746-CIBER de Enfermedades Raras (CIBERER), Instituto de Investigación Sanitaria IdiPAZ, 28049 Madrid, Spain
[b] Pediatric Neurology Department, Hospital Sant Joan de Déu, Institut de Recerca Sant Joan de Déu, 08950 Barcelona, Spain
[c] U-703 Centre for Biomedical Research on Rare Diseases (CIBER-ER), Instituto de Salud Carlos III, Spain
[d] Department of Molecular Biology and Biochemistry, University of Málaga, Málaga, Spain
[e] U-741, CIBER de Enfermedades Raras (CIBERER), Instituto de Salud Carlos III, Madrid, Spain
[f] The Biomedical Research Institute of Málaga (IBIMA), Málaga, Spain
[g] Spanish National Bioinformatics Institute (INB/ELIXIR-ES), Madrid, Spain

ARTICLE INFO

Keywords:
PMM2-CDG
Patient-derived fibroblasts
Transcriptomics
Systems biology
Pharmacological chaperones
Drug repurposing
RNA-seq

ABSTRACT

PMM2-CDG (MIM # 212065), the most common congenital disorder of glycosylation, is caused by the deficiency of phosphomannomutase 2 (PMM2). It is a multisystemic disease of variable severity that particularly affects the nervous system; however, its molecular pathophysiology remains poorly understood. Currently, there is no effective treatment. We performed an RNA-seq based transcriptomic study using patient-derived fibroblasts to gain insight into the mechanisms underlying the clinical symptomatology and to identify druggable targets. Systems biology methods were used to identify cellular pathways potentially affected by PMM2 deficiency, including *Senescence*, *Bone regulation*, *Cell adhesion and Extracellular Matrix (ECM)* and *Response to cytokines*. Functional validation assays using patients' fibroblasts revealed defects related to cell proliferation, cell cycle, the composition of the ECM and cell migration, and showed a potential role of the inflammatory response in the pathophysiology of the disease. Furthermore, treatment with a previously described pharmacological chaperone reverted the differential expression of some of the dysregulated genes. The results presented from transcriptomic data might serve as a platform for identifying therapeutic targets for PMM2-CDG, as well as for monitoring the effectiveness of therapeutic strategies, including pharmacological candidates and mannose-1-P, drug repurposing.

1. Introduction

Protein glycosylation, which involves the covalent attachment of glycans to the polypeptide chains, is one of the most important post-translational modifications of proteins and contributes to their folding, stability, transport, and function. Glycoproteins account for approximately half of the proteins typically expressed in a cell and are involved in a wide variety of cellular and physiological processes [1].

Congenital disorders of glycosylation (CDGs) comprise a growing family of rare metabolic diseases resulting from genetic defects affecting the synthesis, attachment, and transport of glycoconjugates [2]. The most common form, PMM2-CDG, is caused by the deficiency of the enzyme phosphomannomutase 2 (PMM2), which catalyzes the conversion of mannose-6-phosphate into mannose-1-phosphate in one of the initial steps of the N-glycosylation pathway. Clinical phenotypes are variable, ranging from mild to severe with neonatal death. Nearly all patients show neurological symptoms, such as inability to walk, lack of speech, intellectual disability, cerebellar atrophy, epilepsy, strabismus, and stroke-like episodes. Other clinical features commonly reported include failure to thrive, hypotonia, liver disease, immune dysfunction, coagulopathy, skeletal abnormalities, and endocrinological manifestations [3].

* Correspondence to: J.A.G. Ranea, Department of Molecular Biology and Biochemistry, University of Málaga, Málaga, Spain.
** Corresponding author. Centro de Diagnóstico de Enfermedades Moleculares, Centro de Biología Molecular-SO UAM-CSIC, Universidad Autónoma de Madrid, Campus de Cantoblanco, U746-CIBER de Enfermedades Raras (CIBERER), Instituto de Investigación Sanitaria IdiPAZ, 28049 Madrid, Spain.
E-mail addresses: ranea@uma.es (J.A.G. Ranea), bperez@cbm.csic.es, belen.perez@uam.es (B. Pérez).

https://doi.org/10.1016/j.bbadis.2024.167163
Received 22 November 2023; Received in revised form 15 March 2024; Accepted 4 April 2024
Available online 8 April 2024
0925-4439/© 2024 The Authors. Published by Elsevier B.V. This is an open access article under the CC BY license (http://creativecommons.org/licenses/by/4.0/).

Despite many attempts from the scientific community, there is still no curative treatment available for PMM2-CDG and only supportive therapies can be provided to sufferers [2]. Given the disabling and life-threatening effects of this orphan disease, there is an urgent need for research focused on improving treatment options. Our group has contributed to the development of proof-of-concept strategies using small molecules such as pharmacological chaperones (PCs) and proteostasis regulators (PR) [4,5]. These compounds aim to rescue the enzymatic activity of the PMM2 protein in cases where pathogenic variants affect its folding and stability [6,7]. More specifically, our group has identified the hit candidate PC 1-(3-chlorophenyl)-3,3-bis (pyridin-2-yl)-urea, named "compound VIII".

One way to search for better treatments for disease is to exploit current knowledge of the pathophysiology and the molecular mechanisms responsible for the clinical symptoms. This can help drug repurposing, which relies on the identification of novel medical indications for approved or investigational drugs with known safety profiles. Some commercially available drugs have been successfully tested for the treatment of PMM2-CDG following this approach [8,9].

A better understanding of the cellular pathways disrupted by PMM2 deficiency will be crucial if we are to reveal the link between glycosylation defects and patients' phenotypes. The expanding use of "omic" techniques (i.e., phenomics, genomics, transcriptomics, proteomics, and metabolomics) allows us to collect a large amount of data related to molecular processes, providing biological insight into the specific signalling pathways underlying normal and diseased states [10].

Systems biology approaches integrate omic data, employing artificial intelligence and machine learning methods to generate computational models capable of identifying molecular patterns associated with disease [11]. Many aspects of preclinical research for the treatment of PMM2-CDG can benefit from these approaches, such as the discovery of target pathways for pharmacological modulation as well as novel, suitable biomarkers to monitor disease progression and response to potential therapies. Computational approximations can also be applied to boost drug repurposing by finding new relationships between candidate compounds and altered cellular pathways [12].

Transcriptomic analysis based on RNA sequencing (RNA-seq) is one of the most well established omic-based strategies for investigating disease molecular signatures [13]. An altered gene expression profile could contribute to the pathogenesis of PMM2-CDG, as was suggested in a recent study performing RNA microarray analysis on patient-derived B cells [14]. Furthermore, it provides an opportunity for therapeutic assessment based on the correction of the transcriptomic signature towards a normal state [15].

Herein, we present the transcriptomic analysis of PMM2-CDG patient-derived fibroblasts using RNA-seq. Our aim was to identify differentially expressed genes (DEGs) associated with the pathophysiology of the disease and explore the effect of the PC compound VIII on the transcriptomic profile. These DEGs were used to generate a bioinformatic model of the disease by applying systems biology methods to gain deeper knowledge of the affected biological pathways. We identified 17 cellular motives potentially affected by PMM2 deficiency, highlighting *Senescence*, *Bone regulation*, *Cell adhesion and extracellular matrix* and *Response to cytokines*, which were validated by functional assays. The results presented in this work could be exploited to identify potential therapeutic targets for this orphan disease.

2. Materials and methods

2.1. Patient and sample collection

A cohort of 12 PMM2-CDG patients (9 males and 3 females) carrying variants potentially responsive to treatment with PC [4,6] was included in this work. Their phenotypes were evaluated according to 59 items and three clinical indexes, including dysmorphological features and medical comorbidities in the different medical areas. Findings were encoded using Human Phenotype Ontology (HPO) terms [16] where possible. Complementary exploration results and a clinical score assessment have also been included. Clinical and molecular data is included in Supplementary Table S1. Severity categorization of patients into three subsets based on phenotypes was performed using the Nijmegen Pediatric CDG Rating Score (NPCRS), the International Cooperative Ataxia Rating Scale (ICARS), and the midsagittal relative vermis diameter (MVRD) in the magnetic resonance imaging [17]. All the experimental protocols followed in the present study were approved by the Institutional Ethics Committee of the Universidad Autónoma de Madrid. Adhering to Spanish and European Union legislation, informed consent was obtained from the patients' legal guardians.

Commercially available fibroblasts derived from 5 healthy individuals were used as control cell lines. All the cell lines used in the study are summarized in Table 1.

2.2. Cell culture

Control and patient-derived fibroblasts were grown under standard conditions in minimal essential medium (MEM) supplemented with 1 % glutamine, 10 % fetal calf serum (FCS), and antibiotics. Cells were synchronized by FCS deprivation (MEM 1 % glutamine, 0.5 % FCS and antibiotics) for 48 h, followed by 24 h of standard medium before the extraction of RNA or protein or further experiments. To assess the effect of the PC, synchronized fibroblasts from the C1, C2, C3, P6, P7 and P9 lines were treated with 10 μM of 1-(3-chlorophenyl)-3,3-bis(pyridin-2-yl)-urea (referred to as compound VIII) for 48 h.

2.3. RNA-seq analysis

For RNA extraction, 10^6 fibroblasts were seeded in T25 flasks and synchronized by FCS deprivation to reduce bias in gene expression. Cells were harvested by trypsinization, and total RNA was isolated using RNeasy Micro Kit (Qiagen) according to the manufacturer's instructions.

Prior to sequencing, the quality of the obtained RNA was evaluated using a 2100 Bioanalyzer (Agilent Technologies, USA). Only samples with RNA Integrity Numbers >8 were used for further study. Two separate RNA-seq experiments were performed. The first, pilot RNA-seq included the RNA samples from control lines C1, C2 and C3 and patient lines P6, P7 and P9, all of them untreated and treated with compound VIII, which were sequenced using a HiSeq 2500 platform (Illumina, USA). For the second experiment, the RNA samples from all 5 healthy control and 12 PMM2-CDG lines were sequenced using the NovaSeq 6000 system (Illumina, USA).

The RNA-seq samples from both experiments were pre-processed using SeqtrimBB (https://github.com/rafnunser/seqtrimbb.git) and reads were mapped to the human genome (version GRCh38) with STAR (v2.5.3), using an in-house workflow produced with the workflow manager AutoFlow, to obtain tables of counts of mapped reads per sample. Gene expression analysis was performed using the script degenes_hunter.R, from the ExpHunterSuite Pipeline [18], to detect differentially expressed genes by applying the edgeR, limma and DESeq2 algorithms. Differentially expressed genes were those detected by at least two packages with absolute log base 2 fold change values (log2FC) > 1 and False Discovery Rate (FDR) values <0.05.

The different comparisons performed to analyze the RNA-seq data, as well as the samples included in each group, are summarized in Table 2. The functions of the differentially expressed genes were investigated using over representation analysis to look for enriched Gene Ontology (GO) terms, and Kyoto Encyclopedia of Genes and Genomes (KEGG) and Reactome pathways, using the script functional_hunter.R with an FDR $<$ 0.1.

2.4. Therapeutic performance mapping system analysis

Therapeutic Performance Mapping System (TPMS) technology [19]

Table 1
Control and PMM2-CDG patients' lines included in the RNA-seq studies.

Sample	Code nome	Reference/pathogenic variants		Gender	Phenotype	RNA-seq experiments	
						Pilot study	Validation study
Control	C1	CC2509 (Lonza)		M	Healthy	Yes	Yes
Control	C2	CC2511 (Lonza)		M	Healthy	Yes	Yes
Control	C3	GM8429 (Coriell Institute)		M	Healthy	Yes	Yes
Control	C4	GM8447 (Coriell Institute)		F	Healthy		Yes
Control	C5	GM9503 (Coriell Insitute)		M	Healthy		Yes
Patient	P1	p.Thr237Met	p.Thr237Met	M	Mild		Yes
Patient	P2	c.256-1G > T	p.Leu32Arg	F	Mild		Yes
Patient	P3	p.Arg141His	p.Cys241Ser	M	Mild		Yes
Patient	P4	p.Arg141His	p.Leu32Arg	M	Mild		Yes
Patient	P5	c.523+3A>G	p.Arg162Trp	M	Mild		Yes
Patient	P6	c.640-9 T > G	p.Thr237Met	F	Moderate	Yes	Yes
Patient	P7[a]	p.Arg141His	p.Arg162Trp	F	Unclassified	Yes	Yes
Patient	P8	p.Arg141His	p.Thr237Met	M	Severe		Yes
Patient	P9	p.Arg141His	p.Asp65Tyr	M	Severe	Yes	Yes
Patient	P10	p.Arg141His	p.Tyr64Cys	M	Severe		Yes
Patient	P11	p.Phe207Ser	p.Glu139Lys	M	Severe		Yes
Patient	P12	p.Pro113Leu	p.Thr237Lys	M	Severe		Yes

[a] P7 was not able for phenotyping.

Table 2
Summary of the comparisons and the samples included within each group for both RNA-seq experiments.

RNA-seq experiment	Comparison	Samples included in each group	
		Group 1	Group 2
Pilot study	Control vs. patient lines	C1, C2, C3	P6, P7, P9
Pilot study	Untreated vs PC-treated control lines	Untreated C1-C3	PC-treated C1-C3
Pilot study	Untreated vs. PC-treated patient lines	Untreated P6, P7 and P9	PC-treated P6, P7 and P9
Validation study	Control vs. all patient lines	C1 - C5	P1 - P12
Validation study	Control vs. severe patient lines	C1 - C5	P8 - P12
Validation study	Mild patient lines vs. severe patient lines	P1 - P5	P8 - P12

was applied to build a model of PMM2-CDG from the transcriptomic data. For this, the results of the functional enrichment analysis were used to define a list of cellular motives involved in the disease. Once these processes were defined, GO biological processes were used to retrieve a list of proteins, and only those that were differentially expressed according to the transcriptomic data were included in the molecular characterization of the disease. These were known as PMM2-CDG-associated motives.

For the generation of the mathematical model, a biological map was built including all proteins in the human proteome. The map was extended by adding knowledge-oriented connectivity layers, such as protein-to-protein interactions, signalling, metabolic relationships, and gene expression regulation. Data was obtained from public and private external databases (KEGG, Reactome, BioGRID, Intact) as well as through manual curation of scientific literature.

Once the mathematical model was generated, its predictive power was exploited through an ANN strategy [20] to rank the list of DEGs according to their relationship with PMM2-CDG-associated motives, prioritizing those predicted to have a strong relationship (ANN score > 78 %, $p < 0.05$) or a medium-strong relationship (ANN score 71–78 %, $p < 0.1$).

2.5. Functional studies

Fibroblasts from three control lines (C1, C2 and C3) and three PMM2 lines (P6, P7 and P9) were used to conduct functional assays to validate the transcriptomic data.

2.5.1. RT-qPCR

Differential expression data were validated by RT-qPCR. cDNA was synthetized from 250 or 500 ng of total RNA using the NZY First-Strand cDNA Synthesis Kit (Nzytech, Portugal) and amplified with the PerfeCTa SYBR Green FastMix (Quanta Biosciences, USA) and a LightCycler®480 device (Roche Applied Sciences, Germany). *GAPDH* expression was used as an endogenous control. The raw threshold cycle (Ct) values were determined, and relative quantification was analyzed according to the $2^{-\Delta\Delta Ct}$ method.

2.5.2. Western blot

For protein analysis, fibroblasts were grown in T25 flasks and harvested with trypsin. Total protein was extracted using lysis buffer (0.1 % triton, 10 % glycerol, 150 mM NaCl, 10 mM Tris HCl pH 7.5) containing Complete Mini EDTA-free Protease Inhibitor Cocktail (Roche Applied Sciences, Germany) and nitrogen freeze-thaw cycles. After quantifying the concentration of soluble fraction by Bradford assay (BioRad, USA), 50 μg of total protein were subjected to electrophoresis in 4–12 % NuPAGE Novex Bis–Tris precast polyacrylamide gel (Invitrogen). Proteins were transferred to a nitrocellulose membrane using the iBlot 2 Dry blotting system (Invitrogen). After 1 h of blocking with Tris-buffered saline (TBS) containing 5 % non–fat dry milk and 0.1 % Tween–20, immunodetection was performed using commercially available primary antibodies against Palladin (1:1000, Proteintech), Nexilin (1:1000, Abcam) and Cyclooxygenase 2 (1:1000, Invitrogen). Anti-rabbit (1:5000, Cell Signalling) and anti-mouse (1:2000, Cell Signalling) were employed as secondary antibodies. β-actin (1:5000, Abcam) was used as a loading control to normalize the amount of protein. Protein bands were detected with SuperSignal™ West Femto Maximum Sensitivity Substrate (ThermoFisher Scientific). The films were scanned and analyzed using the GS − 900 Calibrated Densitometer (BioRad) and the ImageLab software (BioRad).

2.5.3. Cell cycle analysis

Fibroblasts were harvested by trypsinization, washed in ice-cold PBS and fixed in 70 % ethanol at 4 °C for 18 h. After fixation, the cells were washed in PBS and incubated with propidium iodide/RNase staining buffer (BD Biosciences) for 30 min. The DNA content of the stained cells was analyzed by flow cytometry using a FACSCalibur system (BD Biosciences, USA).

2.5.4. Proliferation assay

Cell proliferation was evaluated through a CCK8 assay (Abcam) following the manufacturer's instructions. Fibroblasts were seeded into a

96-well plate at 5000 cells/well and grown overnight. CCK8 reagent was added to the culture medium at 24, 48, 72 and 96 h after seeding to reach a final concentration of 10 %. After 2 h of incubation at 37 °C, absorbance at 450 nm was measured to assess the generation of the formazan product by viable cells.

2.5.5. Wound healing assay

Fibroblasts from C1, P6, P7 and P9 lines were grown to confluence in 6-well plates and starved in serum-free medium for 24 h before the wounding. A sterile 200 μL pipette tip was used to create a scratch in the cell monolayer. The migration of cells was monitored using an inverted microscope and images were taken over the next 17 h (at 1 frame/20 min) using time-lapse microscopy. The images were analyzed using ImageJ software to measure the distance between the wound edges at each time point.

2.6. Statistics analysis

Prism 8 (GraphPad Software Inc.) was used for statistical analyses of functional assays. Data were expressed as mean ± SD. Statistical significance was determined using unpaired 2-tailed Student's *t*-test with Welch's correction. A P value of <0.05 was considered statistically significant.

3. Results

3.1. Transcriptomic analysis of PMM2-CDG derived fibroblasts reveals affected pathways

To identify disease related cellular pathways we conducted a transcriptomic analysis of fibroblasts derived from 12 PMM2-CDG patients classified according to disease severity. This cohort included 5 severe cases, 1 moderate, 5 mild and 1 unclassified, representative of the previously reported variability in patient phenotypes for this disorder.

We first performed a pilot RNA-seq experiment to obtain transcriptomic data from three healthy control individuals and three PMM2-CDG patients. After the differential expression analysis using the ExpHunter Suite methodology [18] we were able to detect 409 DEGs, of which 257 were downregulated and 152 upregulated (FDR < 0.05 and absolute log2FC > 1). To assess the biological relevance of the DEGs identified, functional enrichment analysis was performed using KEGG, GO and Reactome. The results showed the statistically significant dysregulation of genes involved in pathways related to morphogenesis and development of tissues, the structure and organization of the extracellular matrix (ECM), including the formation of collagen IV networks, and signalling pathways (Wnt, MAPK and tyrosine kinase receptors) (Fig. 1).

To increase power and ensure robust results, we extended the RNA-seq study to include 9 additional PMM2-CDG cases and a total of 5 healthy control lines. We detected 315 DEGs when comparing all PMM2 lines to the controls. We identified 345 DEGs in the cells from the severe patients compared to the controls and 23 DEGs in the cells from the severe patients compared to the milder ones.

For the *control* vs. *all patient lines* and *control* vs. *severe patient lines* comparisons, functional enrichment analysis of the transcriptomic data revealed an involvement of pathways related to the organization and composition of the ECM, cell adhesion, cell cycle, actin cytoskeleton and signalling cascades responsible for cell differentiation, organ morphogenesis and development, validating the results of the pilot project (Supplementary Fig. S1). Table 3 shows the 10 DEGs with highest positive and negative log FC values, with the associated FDR values and a short summary of their functions. In order to validate the RNA-seq data, this set of 20 DEGs was analyzed by RT-qPCR using three control and three patient cell lines. We found significant changes for 15 of the 20 genes evaluated (Fig. 2).

3.2. Senescence, bone regulation, cell adhesion and ECM and response to cytokines are affected motives in PMM2-CDG fibroblasts

TPMS technology was applied to integrate the transcriptomic data from the different RNA-seq datasets into a computational model of the disease based on artificial intelligence and pattern recognition techniques. This methodology led to 17 cellular processes (named motives) that could contribute to the development of PMM2-CDG symptoms (Supplementary Table S2). Most of these were related to the synthesis, modification and degradation of proteins, the response to stimuli and different signalling pathways.

To gain insight into the pathophysiological processes predicted to be affected in PMM2-CDG, we further investigated some of the motives identified by the computational model using functional validation assays. *Senescence*, *Bone Regulation*, *Cell adhesion and ECM* and *Response to Cytokines* were selected based on their relationship with the symptomatology, their novelty, and their relevance within the model (number of DEGs predicted to have a strong relationship with the motive, fold change of the candidate genes and potential targets for therapeutic drug testing).

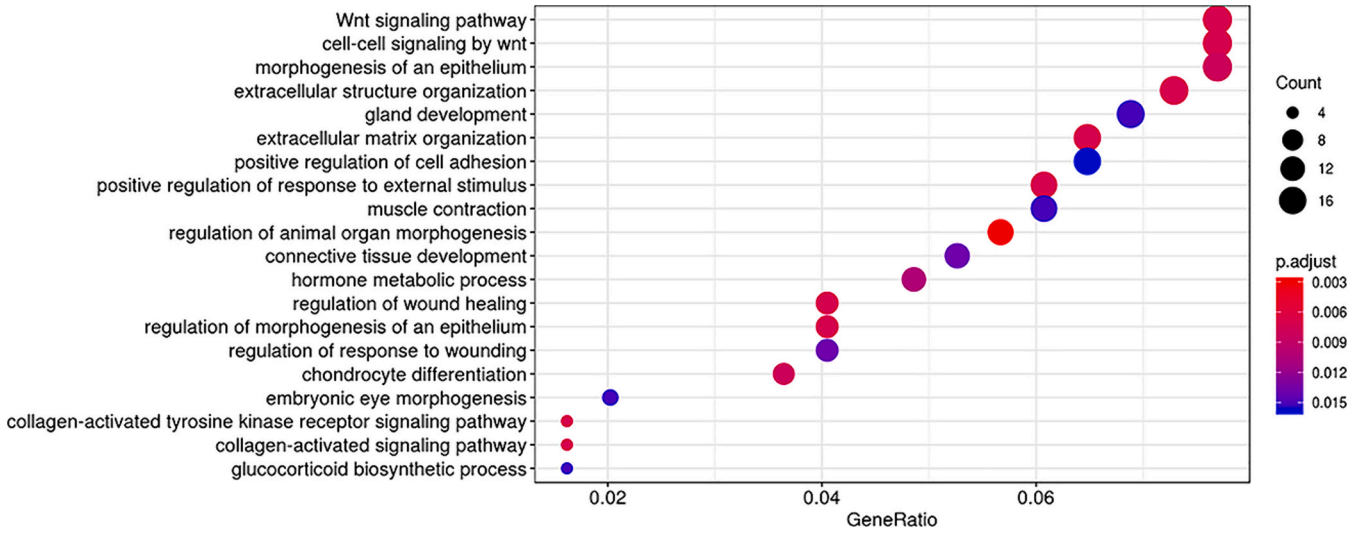

Fig. 1. Functional enrichment analysis of the pilot RNA-seq study. The plot shows the top functional terms in descending order according to gene ratio. The color represents the associated adjusted *p*-value. The X axis represents the gene ratio and the dot size the number of DEGs associated with the functional term.

Table 3
Top 20 under- and overexpressed genes in PMM2 fibroblasts.

Gene	Protein	Log2 FC	FDR	Function
MAB21L2	Protein mab-21-like 2	−9,00	2,3E-13	Embryonic development
ALDH1A1	Retinal dehydrogenase 1	−8,70	1,3E-04	Fructose catabolic process
KRT17	Keratin-17	−8,00	1,8E-07	Hair follicle morphogenesis
COL22A1	Collagen alpha-1(XXII) chain	−7,26	8,3E-17	Endothelial cell morphogenesis
GBX2	Homeobox protein GBX-2	−7,18	5,8E-06	Hindbrain development
NPPB	Natriuretic peptides B	−6,94	1,8E-06	Positive regulation of renal sodium excretion
ADGRL3	Adhesion G protein-coupled receptor L3	−6,72	5,0E-12	Cell-cell adhesion and neuron guidance
BEX1	Brain-expressed X-linked protein 1	−6,63	7,6E-16	Nervous system development
CCDC190	Coiled-coil domain-containing protein 190	−6,39	3,3E-05	Unclassified
NUP210	Nuclear pore membrane glycoprotein 210	−5,97	3,15E-07	Nuclear pore assembly and fusion
CNKSR2	Connector enhancer of kinase suppressor of ras 2	3,60	1,1E-04	Intracellular signal transduction
THBS4	Thrombospondin-4	3,85	1,0E-04	Endothelial cell-cell adhesion
PLXDC2	Plexin domain-containing protein 2	3,87	2,1E-07	Unclassified
ZIC4	Zinc finger protein ZIC 4	4,19	2,6E-10	Central nervous system development
FXYD6	FXYD domain-containing ion transport regulator 6	4,46	8,3E-05	Ion transmembrane transport
ZIC1	Zinc finger protein ZIC 1	4,51	1,2E-10	Positive regulation of protein import into nucleus
NRK	Nicotinamide riboside kinase 1	4,67	2,6E-02	Regulation of cell population proliferation
ADAMTSL3	ADAMTS-like protein 3	5,57	2,8E-06	Extracellular matrix organization
GALNT13	Polypeptide *N*-acetylgalactosaminyltransferase 13	5,64	8,9E-07	Protein O-linked glycosylation
CHN2	Beta-chimaerin	5,84	6,6E-05	Intracellular signal transduction

According to the ANN analysis, 24 DEGs were predicted to have a strong or medium-strong relationship with the *Senescence* motive. Most of the DEGs with decreased expression in the patients' cells play different roles in the progression of cell cycle, including *CCNA2*, *CCNB1*, *CCNB2*, *CDK6* and *HMGA2*. Among the over-expressed genes, the most strongly related were *GADD45G* and *DDIT3*, involved in the induction of cell cycle arrest in response to stress. Supplementary Table S3 shows the entire list of candidates with a brief description of their functions.

In order to validate this motive, the proliferative ability of PMM2 fibroblasts was investigated through a CCK8 assay and their cell cycle was evaluated by flow cytometry. The results showed a significant reduction of 42.1 % and 50.3 % at 48 h and 72 h respectively in the proliferation rate of patients' fibroblasts compared to control lines. Regarding the cell cycle analysis, a significantly higher percentage of patients' cells were found at the G0/G1 phase, while the percentage of cells at the G2/M phase was higher for control lines (Fig. 3 and B). No significant differences were observed for S phase.

Regarding *Bone Regulation*, the genes predicted to have the strongest relationship with this motive encode proteins belonging to the collagen IV and laminin families (Table S3). The expression levels of the genes *COL4A1*, *COL4A2*, *COL4A5* and *COL4A6* (collagen IV isoforms) and *LAMA3* and *LAMA5* (isoforms of laminin-α) were decreased in PMM2 fibroblasts according to the RNA-seq results. *LAMC2* and *LAMC3* (laminin-γ) showed reduced expression levels and *COL4A4* showed increased expression levels in the validation cohort only. RT-qPCR was performed to validate the RNA-seq observations, confirming differential expression for all genes except *LAMA5* and *LAMC2* (Fig. 3C).

According to the ANN analysis, 9 DEGs were predicted to have a strong relationship with the *Cell adhesion and ECM* motive (Table S3). Two of the down-regulated DEGs, *PALLD* and *NEXN*, encode the actin binding proteins palladin and nexilin respectively and have been proposed to contribute to the process of cell motility [21,22]. Their differential expression was validated by RT-qPCR and western blot in the six fibroblast cell lines from the pilot project, confirming a significant decrease in patient-derived cells (Fig. 3D).

To further investigate a possible alteration in the migration ability of patients' cells, we conducted a wound healing assay to analyze the closure rate of a gap caused by a scratch in the fibroblast monolayer. The analysis of time-lapse images taken over 17 h revealed a reduction in the collective motion speed of the PMM2 cells compared to control fibroblasts (Fig. 3E).

Finally, we evaluated the motive *Response to Cytokines*, which showed the greatest number of strongly related DEGs within the model, including genes encoding growth factors, receptors, cell adhesion molecules, and other signalling proteins related to the immune response (Table S3). Among them, we focused on the up-regulated gene *PTGS2*, which encodes the protein cyclooxygenase 2 (COX-2). COX-2 plays a central role in the induction of the inflammatory response as the rate-limiting enzyme in the biosynthesis pathway of prostaglandins. [23] Western blot analysis of fibroblasts cell lines showed increased levels of COX-2 protein in the patient-derived cells (Fig. 3F).

3.3. Pharmacological chaperone treatment in PMM2 fibroblasts

To establish a proof of concept regarding the use of PCs for the treatment of PMM2-CDG, we conducted an RNA-seq analysis to evaluate the effects of compound VIII on the transcriptome of three PMM2 fibroblast lines. The differential expression analysis revealed 206 DEGs in the PMM2 cells upon treatment with compound VIII compared to the untreated ones. Notably, 56 DEGs overlapped with the comparison between control and patient lines, and 50 of them showed reversed expression patterns, suggesting a partial restoration of the transcriptomic phenotype (Fig. 4A). The 50 DEGs, along with a brief description of their functions, are detailed in Supplementary Table S4. 33 down-regulated genes in the PMM2 cells previously compared to the control lines increased their expression after treatment with the chaperone. According to the functional enrichment analysis, most of them were involved in the progression and regulation of the cell cycle and the processes of DNA replication and repair. Furthermore, 17 genes over-expressed in the PMM2 cells, mainly involved in signalling pathways related to the immune response, were downregulated after treatment (Fig. 4B). Interestingly, no significant DEGs were detected in the control cell lines treated with the chaperone.

The 50 genes showing a reversion of their differential expression upon treatment with the PC were also included in the ANN analysis. Out of them, 11 showed a strong relationship with at least one motive, highlighting the motives *Senescence*, *Golgi and protein trafficking*, *Response to cytokines* or *MAPK pathway* (Supplementary Table S4).

4. Discussion

Despite the valuable efforts of the scientific community, there are still significant obstacles that need to be addressed to develop effective therapies for PMM2-CDG, the most common congenital disorder of glycosylation, including a lack of knowledge about the mechanisms that link the molecular defect with the clinical symptomatology. In this work, we conducted a transcriptomic analysis of patient-derived fibroblasts to gain insight into the underlying pathophysiology of this orphan disease.

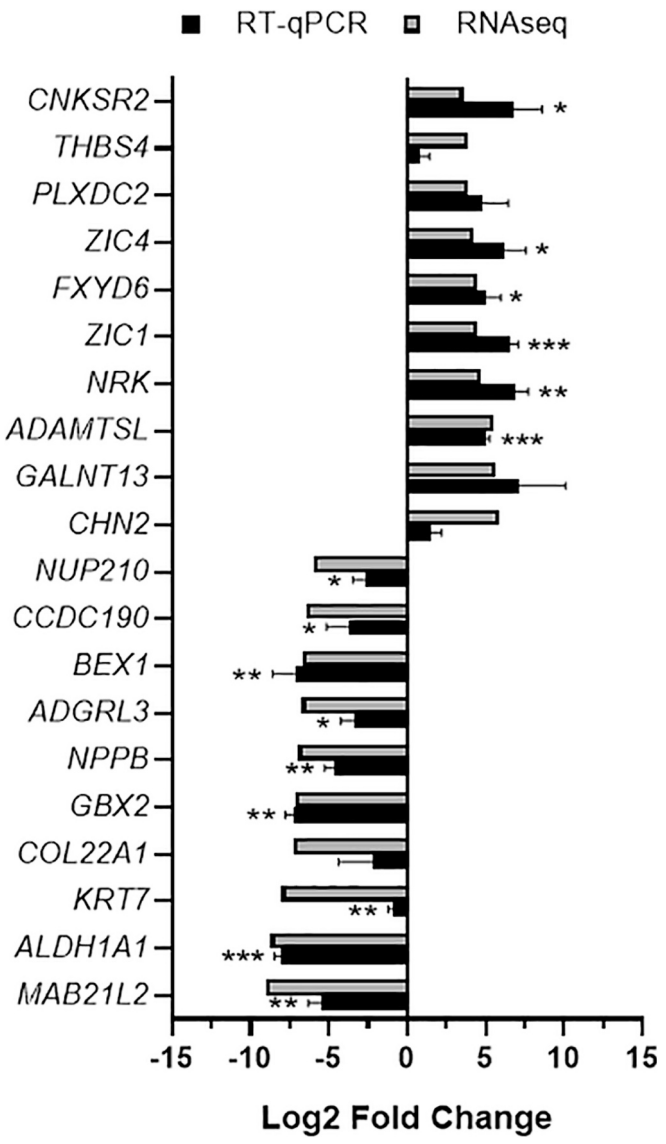

Fig. 2. Validation of the DEGs by RT-qPCR. Bar chart shows the Log2 FC for the 20 most differentially expressed genes in PMM2 cells determined by RT-qPCR and the equivalent RNA-seq results. *GAPDH* was used as endogenous control. $^{*}p < 0.05$, $^{**}p < 0.01$, $^{***}p < 0.001$.

Furthermore, taking advantage of artificial intelligence-based tools and pattern recognition techniques, transcriptomic data were used to build a computational model of the disease, identifying potential affected cellular pathways that we validated using functional assays.

Patient-derived fibroblasts from other CDG subtypes have already been used to perform gene expression studies, revealing the dysregulation of genes encoding components of the ECM, including collagen IV [24]. Recent work demonstrated transcriptional alterations in PMM2 deficient B-LCL cells, affecting the expression of regulators of cell differentiation, response to stress, cytokine production, cell adhesion and motility, and other signalling pathways [14]. To our knowledge, our study reports the first transcriptional study carried out in skin fibroblasts derived from PMM2-CDG patients.

The initial RNA-seq experiment allowed us to obtain preliminary insights into the genes that were differentially expressed in fibroblast lines derived from three PMM2-CDG patients. The remarkable consistency with the results of the second RNA-seq, including lines from 12 PMM2-CDG patients of varying disease severity, validated our findings and showed their robustness. In line with previous studies, among the most enriched terms we found pathways related to the morphogenesis and development of tissues, the structure and organization of the ECM, highlighting the formation of collagen IV networks, and signalling pathways. This suggests that some of the underlying pathomechanisms in PMM2-CDG might be conserved across different cell types and could also be shared with other CDGs.

According to this hypothesis, the impairment of different components of the glycosylation machinery could have a similar influence on secondary cellular pathways, regardless of the specific genetic defect. This provides potential opportunities for therapeutic intervention targeting pathways common to different CDGs, increasing the number of patients eligible for novel treatments.

Following a systems biology-based strategy, our transcriptomic data were used to build a computational model of PMM2-CDG. This approach has already been used to gain insight into the pathophysiology of other diseases, such as obesity and amyotrophic lateral sclerosis [25,26]. In our case, the model allowed us to produce a list of 17 affected cellular motives according to the differential expression data, from which we selected *Senescence*, *Bone Regulation*, *Cell adhesion and ECM* and *Response to Cytokines* for further functional validation.

The *Senescence* motive refers to the process of cellular senescence, which implies the irreversible growth arrest in the G0/G1 phase of the cell cycle induced after the exposure of cells to cellular damage or stress [27]. Functional assays showed decreased proliferation rates for patient-derived fibroblasts, along with their arrest in the G0/G1 phase. A reduced proliferative ability of PMM2 deficient fibroblasts has also been reported in previous studies [28]. These results agree with the observed down-regulation of genes encoding the cyclins *CCNA2*, *CCNB1* and *CCNB2* and other regulators (e.g. *CDK6* and *HMGA2*) whose function is required for progression towards the different phases of the cell cycle [29]. Furthermore, *DDIT3*, previously shown to lead to cell cycle arrest in the G1 phase [30], was found significantly up-regulated in the RNA-seq data. *DDIT3* encodes a transcription factor that plays a key role in the stress response. Its expression is induced upon DNA damage, as well as by endoplasmic reticulum (ER) stress and the unfolded protein response (UPR) [30], which are well-documented molecular pathogenesis hallmarks of PMM2-CDG and other CDGs [31].

Cellular senescence has been associated with changes in ECM and collagen homeostasis in the context of aging, revealing a vicious circle in which senescent cells have impaired synthesis of ECM proteins and disruption in ECM homeostasis exacerbates the senescence phenotype [32]. In our study, along with the reduced proliferative ability, PMM2 deficient fibroblasts showed an altered expression of ECM components, highlighting different isoforms of collagen IV and laminin, whose dysregulation was confirmed by RT-qPCR. Collagen IV and laminin are the major components of the basement membrane, a specialised ECM that separates epithelial and endothelial cells from underlying mesenchyme. Pathogenic variants in collagen IV genes lead to multisystemic diseases encompassing eye and kidney defects (including haematuria and proteinuria), stroke-like episodes, seizures, and intracerebral haemorrhage, which are remarkably reminiscent of the clinical presentation of PMM2-CDG patients. At the cellular level, they are also associated with ER stress and the UPR [33].

Some CDG, including PMM2-CDG, exhibit similar characteristics to connective tissue disorders [34]. The ECM is crucial for maintaining the structure and function of connective tissues, such as tendons, ligaments, and cartilage. In the patients included in this study, a combination of connective tissue and skeletal symptoms, including pes planus, joint laxity and scoliosis were observed. Dermatologic issues like peu d'orange, lymphedema, and lipodystrophy are also prevalent in PMM2-CDG, further emphasizing the importance of the ECM in this disorder. The cellular and clinical connection between the ECM and bone regulation is self-evident. For PMM2-CDG, this connection is particularly relevant, as over 85 % of patients in a recently published large series exhibited bone pathology [35]. Guidelines highlight that approximately 60 % of patients have abnormal bone metabolism, resulting in low bone mineral

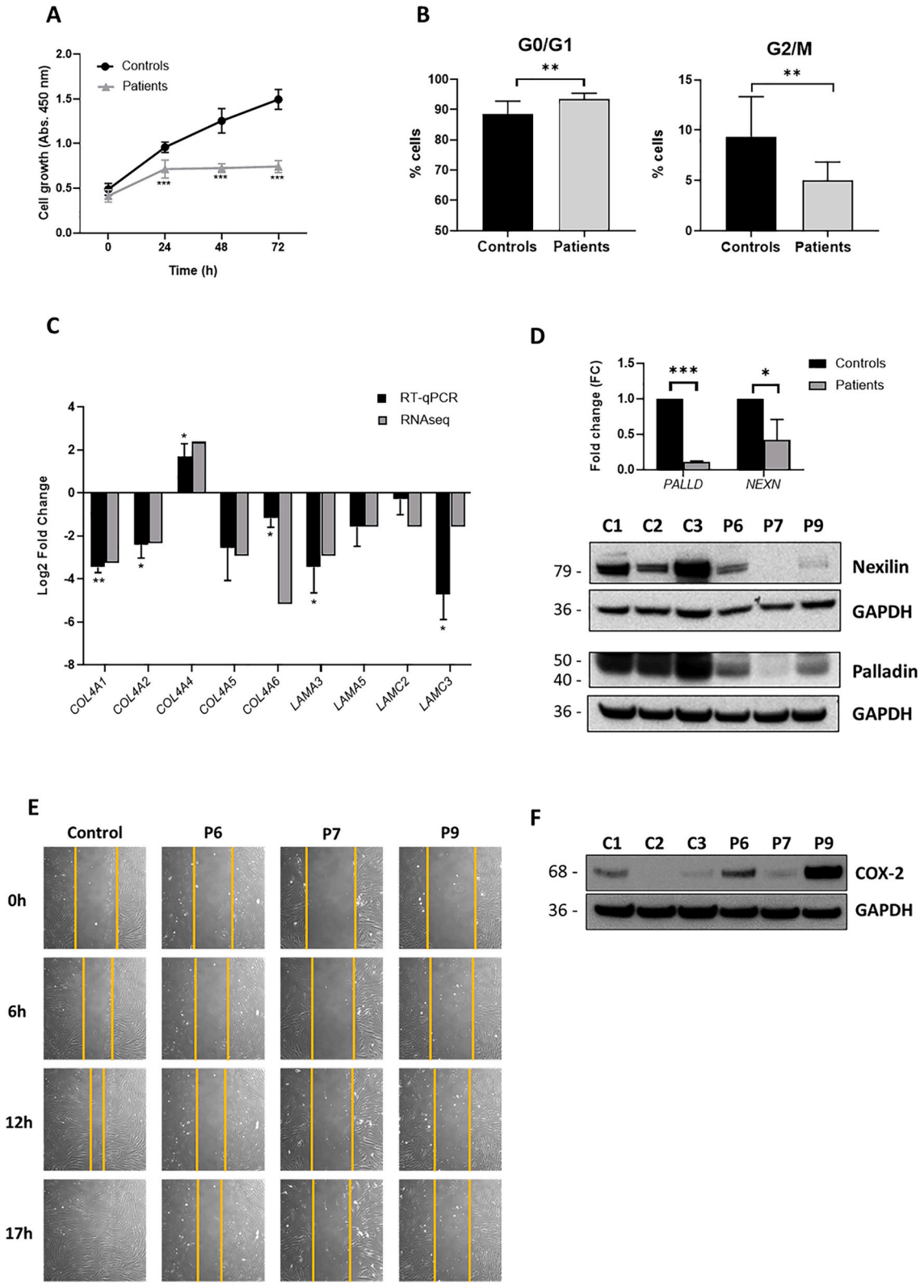

Fig. 3. Functional validation of the *Senescence* (A and B), *Bone regulation* (C), *Cell adhesion and ECM* (D and E) and *Response to cytokines* (F) motives. Patient and health-derived fibroblasts from C1, C2, C3, P6, P7 and P9 lines were used for all functional assays except for the evaluation of migration capability, where we used control (C1) and PMM2 cells (P6, P7 and P9). A) Cell proliferation of control and PMM2 fibroblast lines measured by CCK8 assay at 24, 48 and 72 h. B) Distribution of control and PMM2 cells across the G0/G1 and G2/M phases of cell cycle determined by flow cytometry. Bars represents the percentage of cells in each phase. C) Expression analysis of genes encoding different isoforms of collagen IV and laminin measured by RT-qPCR. Bar shows the Log2 FC for each gene in PMM2 cells alongside the RNA-seq results. *GAPDH* was used as the endogenous control for normalization. D) Analysis of *PALLD* and *NEXN* mRNA and protein levels by RT-qPCR and western blot in control (C1-C3) and PMM2-CDG cells (P6, P7 and P9). GAPDH was used as endogenous control in both experiments. E) Migration capability was evaluated by wound healing assay. Images were taken at 0, 6, 12 and 17 h after the scratch. F) Western blot analysis of COX-2 protein levels in control (C1-C3) and PMM2 cells (P6, P7 and P9). GAPDH was used as endogenous control.

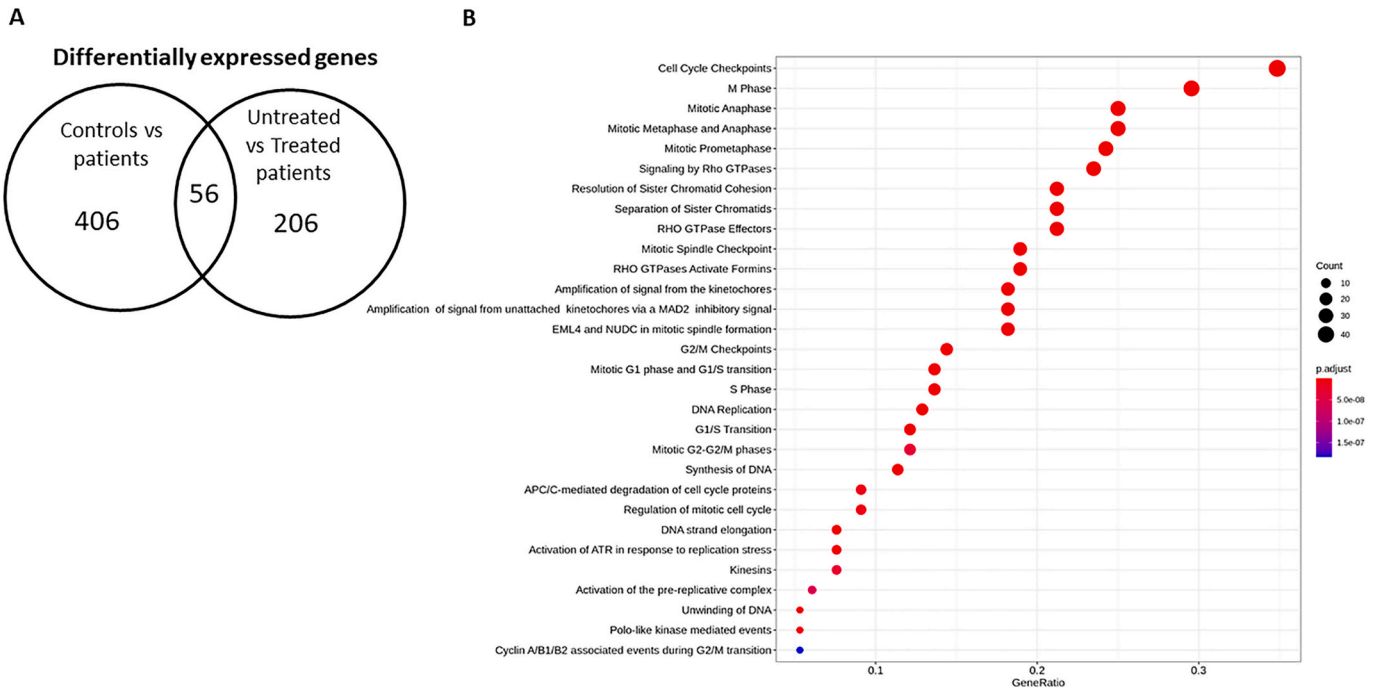

Fig. 4. Effect of the pharmacological chaperone on the transcriptome of PMM2 fibroblasts. A) Venn diagram showing the DEGs in *control* vs *patient lines* and *untreated* vs *treated patient lines*. B) Functional enrichment analysis of DEGs identified in the treated PMM2 cells. The plot shows the top functional terms in descending order according to gene ratio. The color represents the associated adjusted p-value. The X axis represents the gene ratio and the dot size the number of DEGs associated with the functional term.

density ranging from osteopenia to osteoporosis. Consequently, lifelong monitoring and specific therapies are necessary to address this issue [36].

The ECM does not only provide a structural scaffold to the surrounding cells, but also functions as a reservoir of cytokines and growth factors. The interaction between the cells and the ECM, established through cell adhesion structures and strongly dependent on the actin cytoskeleton, is crucial in processes such as cell proliferation and migration [22]. This could explain the decreased migration rates observed in PMM2 deficient fibroblasts.

Finally, for the *Response to cytokines* motive we found dysregulated genes associated with the immune response. The immunological aspect is particularly relevant in PMM2-CDG, since some pediatric patients suffer from recurrent, severe infections, able to trigger stroke-like episodes [37]. Importantly, in reported young patients showing a fatal outcome, infections are, at least partially, the underlying cause of death in many cases. Due to these immunological problems, laboratory investigations should be repeated periodically, especially during infancy, and, according to guidelines, it is crucial to confirm the effectiveness and protective response to vaccines in these individuals [36]. The up-regulation of the COX-2 protein, a key player in prostaglandin synthesis, points to a potential role of the inflammatory response in the pathophysiology of the disease, as has been suggested in previous studies [37]. Fortunately, COX-2 and the inflammatory response have been extensively characterized in the study of other diseases, leading to the development and commercialization of drugs (such as anti-inflammatory agents) that could be repurposed to target this mechanism [38].

Taken together, these results validate the utility of the generated model as a versatile platform for gaining novel insights into the pathophysiology of PMM2-CDG and identifying targetable pathways for therapeutic intervention. Notably, after treating the patients' fibroblasts with the candidate PC we were able to observe a reversion of the differential expression of 50 DEGs. Some of them were involved in the regulation of the cell cycle and DNA replication and repair, including the genes *CCNB1*, *CCNB2* and *HMGA2* mentioned above. This suggests that increasing PMM2 activity in patient-derived fibroblasts may lead to an enhancement in their proliferative capacity. Although the transcriptomic analysis did not reveal an improvement of other genes whose dysregulation was validated through functional assays, we cannot completely rule out that a restoration of PMM2 activity may lead to a recovery of the cellular pathways in which they are involved. Indeed, certain genes related to the inflammatory response are recovered after the treatment with the PC. This is the case of *PLA2G2A*, encoding the secretory phospholipase A2, which acts upstream COX2 in the prostaglandin synthesis pathway. In future investigations, it would be beneficial to specifically evaluate the potential recovery of these pathways by adjusting the dosage or duration of treatment with PC or alternative therapeutic approaches.

This pipeline provides an approach for monitoring and evaluating the effectiveness of treatments aimed at restoring phosphomannomutase activity, such as novel, optimized small chemical drugs (PCs or PRs) and mRNA-based therapies, among others. A similar strategy has already been employed for other metabolic diseases [39]. Furthermore, by deciphering the molecular networks underlying the pathophysiology of the disease, our model may help us to find new treatment options following a repurposing strategy. Drug repurposing holds the potential to mitigate the costs and risks associated with the traditional drug discovery process, making it a faster and less expensive alternative for therapeutic development in PMM2-CDG.

In conclusion, this work presents a promising framework for future therapeutic research strategies targeting orphan diseases, such as PMM2-CDG, using patients-derived fibroblasts and systems biology-based approaches. Further studies are needed to validate our findings and test the potential therapeutic candidates in alternative models, such as differentiated cells derived from PMM2 deficient iPSCs, as well as in a viable murine model of the disease, with lower lethality than the currently available one [40].

Funding statement

This work was funded the Instituto de Salud Carlos (ISCIII), European Regional Development Fund [PI22/00699] to BP. The Spanish Ministry of Economy and Competitiveness (grants PID2019-108096RB-C21 and PID2022-140047OB-C21), the Institute of Health Carlos III (project IMPaCT-Data, exp. IMP/00019), co-funded by the European Union, European Regional Development Fund (ERDF, "A way to make Europe"); and the European Union (HORIZON-HLTH-2022-DISEASE-06, Project ID: 101080580) to JAGR. The "CIBER de Enfermedades Raras" is an initiative from the ISCIII (Spain).

CRediT authorship contribution statement

Diana Gallego: Writing – original draft, Methodology, Formal analysis, Conceptualization. **Mercedes Serrano:** Methodology, Formal analysis, Data curation. **Jose Cordoba-Caballero:** Methodology, Formal analysis. **Alejandra Gámez:** Formal analysis, Conceptualization. **Pedro Seoane:** Formal analysis, Data curation, Methodology, Software, Supervision. **James R. Perkins:** Writing – review & editing, Validation, Software, Methodology, Formal analysis, Conceptualization. **Juan A.G. Ranea:** Writing – review & editing, Validation, Funding acquisition, Conceptualization. **Belén Pérez:** Writing – review & editing, Supervision, Investigation, Funding acquisition, Formal analysis, Conceptualization.

Declaration of competing interest

The authors declare no conflict of interest.

Data availability

Data will be made available on request.

Acknowledgement

We wholeheartedly thank the Spanish families affected by PMM2-CDG who actively participated in this research.

Appendix A. Supplementary data

Supplementary data to this article can be found online at https://doi.org/10.1016/j.bbadis.2024.167163.

References

[1] K.T. Schjoldager, Y. Narimatsu, H.J. Joshi, H. Clausen, Global view of human protein glycosylation pathways and functions, Nat. Rev. Mol. Cell Biol. 21 (2020) 729–749, https://doi.org/10.1038/s41580-020-00294-x.
[2] N. Ondruskova, A. Cechova, H. Hansikova, T. Honzik, J. Jaeken, Congenital disorders of glycosylation: still "hot" in 2020, Biochim. Biophys. Acta Gen. Subj. 1865 (2021) 129751, https://doi.org/10.1016/j.bbagen.2020.129751.
[3] S. Grünewald, The clinical spectrum of phosphomannomutase 2 deficiency (CDG-Ia), Biochim. Biophys. Acta (BBA) - Mol. Basis Dis. 1792 (2009) 827–834, https://doi.org/10.1016/j.bbadis.2009.01.003.
[4] P. Yuste-Checa, S. Brasil, A. Gámez, J. Underhaug, L.R. Desviat, M. Ugarte, C. Pérez-Cerdá, A. Martinez, B. Pérez, Pharmacological chaperoning: a potential treatment for PMM2-CDG, Hum. Mutat. 38 (2017) 160–168, https://doi.org/10.1002/humu.23138.
[5] A. Vilas, P. Yuste-Checa, D. Gallego, L.R. Desviat, M. Ugarte, C. Pérez-Cerda, A. Gámez, B. Pérez, Proteostasis regulators as potential rescuers of PMM2 activity, Biochim. Biophys. Acta Mol. basis Dis. 1866 (2020) 165777, https://doi.org/10.1016/j.bbadis.2020.165777.
[6] C. Segovia-Falquina, A. Vilas, F. Leal, F. Del Caño-Ochoa, E.P. Kirk, M. Ugarte, S. Ramón-Maiques, A. Gámez, B. Pérez, A functional platform for the selection of pathogenic variants of PMM2 amenable to rescue via the use of pharmacological chaperones, Hum. Mutat. 43 (2022) 1430–1442, https://doi.org/10.1002/humu.24431.
[7] P. Yuste-Checa, A. Gámez, S. Brasil, L.R. Desviat, M. Ugarte, C. Pérez-Cerdá, B. Pérez, The effects of PMM2-CDG-causing mutations on the folding, activity, and stability of the PMM2 protein, Hum. Mutat. 36 (2015) 851–860, https://doi.org/10.1002/humu.22817.
[8] A.F. Martínez-Monseny, M. Bolasell, L. Callejón-Póo, D. Cuadras, V. Freniche, D. C. Itzep, S. Gassiot, P. Arango, D. Casas-Alba, E. de la Morena, J. Corral, R. Montero, C. Pérez-Cerdá, B. Pérez, R. Artuch, J. Jaeken, M. Serrano, the C.S. Consortium, AZATAX: acetazolamide safety and efficacy in cerebellar syndrome in PMM2 congenital disorder of glycosylation (PMM2-CDG), Ann. Neurol. 85 (2019) 740–751, https://doi.org/10.1002/ana.25457.
[9] S. Iyer, F.S. Sam, N. DiPrimio, G. Preston, J. Verheijen, K. Murthy, Z. Parton, H. Tsang, J. Lao, E. Morava, E.O. Perlstein, Repurposing the aldose reductase inhibitor and diabetic neuropathy drug epalrestat for the congenital disorder of glycosylation PMM2-CDG, Dis. Model. Mech. 12 (2019) dmm040584, https://doi.org/10.1242/dmm.040584.
[10] Y. Hasin, M. Seldin, A. Lusis, Multi-omics approaches to disease, Genome Biol. 18 (2017) 83, https://doi.org/10.1186/s13059-017-1215-1.
[11] G.L. D'Adamo, J.T. Widdop, E.M. Giles, The future is now? Clinical and translational aspects of "omics" technologies, Immunol. Cell Biol. 99 (2021) 168–176, https://doi.org/10.1111/imcb.12404.
[12] P. Zhang, Y. Itan, Biological network approaches and applications in rare disease studies, Genes 10 (2019) 797, https://doi.org/10.3390/genes10100797.
[13] L. Pirhaji, P. Milani, S. Dalin, B.T. Wassie, D.E. Dunn, R.J. Fenster, J. Avila-Pacheco, P. Greengard, C.B. Clish, M. Heiman, D.C. Lo, E. Fraenkel, Identifying therapeutic targets by combining transcriptional data with ordinal clinical measurements, Nat. Commun. 8 (2017) 623, https://doi.org/10.1038/s41467-017-00353-6.
[14] A. Parrado, G. Rubio, M. Serrano, M.E. De la Morena-Barrio, S. Ibáñez-Micó, N. Ruiz-Lafuente, R. Schwartz-Albiez, A. Esteve-Solé, L. Alsina, J. Corral, T. Hernández-Caselles, Dissecting the transcriptional program of phosphomannomutase 2-deficient cells: Lymphoblastoide B cell lines as a valuable model for congenital disorders of glycosylation studies, Glycobiology 32 (2022) 84–100, https://doi.org/10.1093/glycob/cwab087.
[15] R.S. Dhindsa, A.W. Zoghbi, D.K. Krizay, C. Vasavda, D.B. Goldstein, A transcriptome-based drug discovery paradigm for neurodevelopmental disorders, Ann. Neurol. 89 (2021) 199–211, https://doi.org/10.1002/ana.25950.
[16] P. Robinson, S. Mundlos, The human phenotype ontology, Clin. Genet. 77 (2010) 525–534, https://doi.org/10.1111/j.1399-0004.2010.01436.x.
[17] S. Achouitar, M. Mohamed, T. Gardeitchik, S.B. Wortmann, J. Sykut-Cegielska, R. Ensenauer, H.O. de Baulny, K. Ounap, D. Martinelli, M. de Vries, R. McFarland, D. Kouwenberg, M. Theodore, F. Wijburg, S. Grünewald, J. Jaeken, R.A. Wevers, L. Nijtmans, J. Elson, E. Morava, Nijmegen paediatric CDG rating scale: a novel tool to assess disease progression, J. Inherit. Metab. Dis. 34 (2011) 923–927, https://doi.org/10.1007/s10545-011-9325-5.
[18] F.M. Jabato, J. Córdoba-Caballero, E. Rojano, C. Romá-Mateo, P. Sanz, B. Pérez, D. Gallego, P. Seoane, J.A.G. Ranea, J.R. Perkins, Gene expression analysis method integration and co-expression module detection applied to rare glucide metabolism disorders using ExpHunterSuite, Sci. Rep. 11 (2021) 15062, https://doi.org/10.1038/s41598-021-94343-w.
[19] J.M. Mas Benavente, A. Pujol Torras, P. Aloy Calaf, J. Farrés, Methods and Systems for Identifying Molecules or Processes of Biological Interest by Using Knowledge Discovery in Biological Data. https://patentscope.wipo.int/search/en/detail.jsf?docId=WO2011051805, 2011 (accessed July 17, 2023).
[20] C.M. Bishop, Pattern Recognition and Machine Learning, Springer, New York, 2006.
[21] B. Zhu, C. Rippe, J. Holmberg, S. Zeng, L. Perisic, S. Albinsson, U. Hedin, B. Uvelius, K. Swärd, Nexilin/NEXN controls actin polymerization in smooth muscle and is regulated by myocardin family coactivators and YAP, Sci. Rep. 8 (2018) 13025, https://doi.org/10.1038/s41598-018-31328-2.
[22] X.-S. Liu, H.-J. Luo, H. Yang, L. Wang, H. Kong, Y.-E. Jin, F. Wang, M.-M. Gu, Z. Chen, Z.-Y. Lu, Z.-G. Wang, Palladin regulates cell and extracellular matrix interaction through maintaining normal actin cytoskeleton architecture and stabilizing Beta1-integrin, J. Cell. Biochem. 100 (2007) 1288–1300, https://doi.org/10.1002/jcb.21126.
[23] B. Kaur, P. Singh, Inflammation: biochemistry, cellular targets, anti-inflammatory agents and challenges with special emphasis on cyclooxygenase-2, Bioorg. Chem. 121 (2022) 105663, https://doi.org/10.1016/j.bioorg.2022.105663.
[24] M.R. Lecca, C. Maag, E.G. Berger, T. Hennet, Fibrotic response in fibroblasts from congenital disorders of glycosylation, J. Cell. Mol. Med. 15 (2011) 1788–1796, https://doi.org/10.1111/j.1582-4934.2010.01187.x.
[25] M. Gómez-Serrano, E. Camafeita, E. García-Santos, J.A. López, M.A. Rubio, A. Sánchez-Pernaute, A. Torres, J. Vázquez, B. Peral, Proteome-wide alterations on adipose tissue from obese patients as age-, diabetes- and gender-specific hallmarks, Sci. Rep. 6 (2016) 25756, https://doi.org/10.1038/srep25756.
[26] M. Herrando-Grabulosa, R. Mulet, A. Pujol, J.M. Mas, X. Navarro, P. Aloy, M. Coma, C. Casas, Novel neuroprotective multicomponent therapy for amyotrophic lateral sclerosis designed by networked systems, PloS One 11 (2016) e0147626, https://doi.org/10.1371/journal.pone.0147626.
[27] G. Casella, R. Munk, K.M. Kim, Y. Piao, S. De, K. Abdelmohsen, M. Gorospe, Transcriptome signature of cellular senescence, Nucleic Acids Res. 47 (2019) 7294–7305, https://doi.org/10.1093/nar/gkz555.
[28] M. Görlacher, E. Panagiotou, N. Himmelreich, A. Hüllen, L. Beedgen, B. Dimitrov, V. Geiger, M. Zielonka, V. Peters, S. Strahl, J. Vázquez-Jiménez, G. Kerst, C. Thiel, Fatal outcome after heart surgery in PMM2-CDG due to a rare homozygous gene variant with double effects, Mol. Genet. Metab. Rep. 25 (2020) 100673, https://doi.org/10.1016/j.ymgmr.2020.100673.
[29] S. Lim, P. Kaldis, Cdks, cyclins and CKIs: roles beyond cell cycle regulation, Development 140 (2013) 3079–3093, https://doi.org/10.1242/dev.091744.
[30] A. Osman, M. Lindén, T. Österlund, C. Vannas, L. Andersson, M. Escobar, A. Ståhlberg, P. Åman, Identification of genomic binding sites and direct target

genes for the transcription factor DDIT3/CHOP, Exp. Cell Res. 422 (2023) 113418, https://doi.org/10.1016/j.yexcr.2022.113418.
[31] P. Yuste-Checa, A.I. Vega, C. Martín-Higueras, C. Medrano, A. Gámez, L.R. Desviat, M. Ugarte, C. Pérez-Cerdá, B. Pérez, DPAGT1-CDG: functional analysis of disease-causing pathogenic mutations and role of endoplasmic reticulum stress, PloS One 12 (2017) e0179456, https://doi.org/10.1371/journal.pone.0179456.
[32] M. Gerasymchuk, G.I. Robinson, O. Kovalchuk, I. Kovalchuk, Modeling of the senescence-associated phenotype in human skin fibroblasts, Int. J. Mol. Sci. 23 (2022) 7124, https://doi.org/10.3390/ijms23137124.
[33] F.E. Jones, M.A. Bailey, L.S. Murray, Y. Lu, S. McNeilly, U. Schlötzer-Schrehardt, R. Lennon, Y. Sado, D.G. Brownstein, J.J. Mullins, K.E. Kadler, T. Van Agtmael, ER stress and basement membrane defects combine to cause glomerular and tubular renal disease resulting from Col4a1 mutations in mice, Dis. Model. Mech. 9 (2016) 165–176, https://doi.org/10.1242/dmm.021741.
[34] D. Rymen, J. Jaeken, Skin manifestations in CDG, J. Inherit. Metab. Dis. 37 (2014) 699–708, https://doi.org/10.1007/s10545-014-9678-7.
[35] M. Schiff, C. Roda, M.-L. Monin, A. Arion, M. Barth, N. Bednarek, M. Bidet, C. Bloch, N. Boddaert, D. Borgel, A. Brassier, A. Brice, A. Bruneel, R. Buissonnière, B. Chabrol, M.-C. Chevalier, V. Cormier-Daire, C.D. Barace, E.D. Maistre, A. D. Saint-Martin, N. Dorison, V. Drouin-Garraud, T. Dupré, B. Echenne, P. Edery, F. Feillet, I. Fontan, C. Francannet, F. Labarthe, C. Gitiaux, D. Héron, M. Hully, S. Lamoureux, D. Martin-Coignard, C. Mignot, G. Morin, T. Pascreau, O. Pincemaille, M. Polak, A. Roubertie, C. Thauvin-Robinet, A. Toutain, G. Viot, S. Vuillaumier-Barrot, N. Seta, P.D. Lonlay, Clinical, laboratory and molecular findings and long-term follow-up data in 96 French patients with PMM2-CDG (phosphomannomutase 2-congenital disorder of glycosylation) and review of the literature, J. Med. Genet. 54 (2017) 843–851, https://doi.org/10.1136/jmedgenet-2017-104903.
[36] R. Altassan, R. Péanne, J. Jaeken, R. Barone, M. Bidet, D. Borgel, et al., International clinical guidelines for the management of phosphomannomutase 2-congenital disorders of glycosylation: diagnosis, treatment and follow up, J. Inherit. Metab. Dis. 42 (2019) 5–28, https://doi.org/10.1002/JIMD.12024.
[37] M. Monticelli, T. Ferro, J. Jaeken, V. Dos Reis Ferreira, P.A. Videira, Immunological aspects of congenital disorders of glycosylation (CDG): a review, J. Inherit. Metab. Dis. 39 (2016) 765–780, https://doi.org/10.1007/s10545-016-9954-9.
[38] N. Hashemi Goradel, M. Najafi, E. Salehi, B. Farhood, K. Mortezaee, Cyclooxygenase-2 in cancer: a review, J. Cell. Physiol. 234 (2019) 5683–5699, https://doi.org/10.1002/jcp.27411.
[39] R. Manek, Y.V. Zhang, P. Berthelette, M. Hossain, C.S. Cornell, J. Gans, G. Anarat-Cappillino, S. Geller, R. Jackson, D. Yu, K. Singh, S. Ryan, D.S. Bangari, E.Y. Xu, S. R.M. Kyostio-Moore, Blood phenylalanine reduction reverses gene expression changes observed in a mouse model of phenylketonuria, Sci. Rep. 11 (2021) 22886, https://doi.org/10.1038/s41598-021-02267-2.
[40] B. Chan, M. Clasquin, G.A. Smolen, G. Histen, J. Powe, Y. Chen, Z. Lin, C. Lu, Y. Liu, Y. Cang, Z. Yan, Y. Xia, R. Thompson, C. Singleton, M. Dorsch, L. Silverman, S.-S.M. Su, H.H. Freeze, S. Jin, A mouse model of a human congenital disorder of glycosylation caused by loss of PMM2, Hum. Mol. Genet. 25 (2016) 2182–2193, https://doi.org/10.1093/hmg/ddw085.